environmental microbiology

Environmental Microbiology (2021) **23**(10), 6292–6308 doi:10.1111/1462-2920.15768

Special Issue Article

A fungal powdery mildew pathogen induces extensive local and marginal systemic changes in the *Arabidopsis thaliana* microbiota

Paloma Durán,[1,2] Anja Reinstädler,[3] Anna Lisa Rajakrut,[1] Masayoshi Hashimoto,[4] Ruben Garrido-Oter,[1,2*] Paul Schulze-Lefert[1,2*] and Ralph Panstruga[3*]

[1]*Department of Plant-Microbe Interactions, Max Planck Institute for Plant Breeding Research, Carl-von-Linné-Weg 10, Cologne, 50829, Germany.*

[2]*Cluster of Excellence on Plant Sciences, Düsseldorf, 40225, Germany.*

[3]*RWTH Aachen University, Institute for Biology I, Unit of Plant Molecular Cell Biology, Worringerweg 1, Aachen, 52056, Germany.*

[4]*Graduate School of Agricultural and Life Sciences, The University of Tokyo, Tokyo, 113-8657, Japan.*

Summary

Powdery mildew is a foliar disease caused by epiphytically growing obligate biotrophic ascomycete fungi. How powdery mildew colonization affects host resident microbial communities locally and systemically remains poorly explored. We performed powdery mildew (*Golovinomyces orontii*) infection experiments with *Arabidopsis thaliana* grown in either natural soil or a gnotobiotic system and studied the influence of pathogen invasion into standing natural multi-kingdom or synthetic bacterial communities (SynComs). We found that after infection of soil-grown plants, *G. orontii* outcompeted numerous resident leaf-associated fungi while fungal community structure in roots remained unaltered. We further detected a significant shift in foliar but not root-associated bacterial communities in this setup. Pre-colonization of germ-free *A. thaliana* leaves with a bacterial leaf-derived SynCom, followed by *G. orontii* invasion, induced an overall similar shift in the foliar bacterial microbiota and minor changes in the root-associated bacterial assemblage. However, a standing root-derived SynCom in root samples remained robust against foliar infection with *G. orontii*. Although pathogen growth was unaffected by the leaf SynCom, fungal infection caused a twofold increase in leaf bacterial load. Our findings indicate that *G. orontii* infection affects mainly microbial communities in local plant tissue, possibly driven by pathogen-induced changes in source-sink relationships and host immune status.

Received 28 April, 2021; accepted 7 September, 2021. *For correspondence. Tel: +49 241 80 25566; Fax +49 241 80 22637; E-mail panstruga@bio1.rwth-aachen.de. Tel: +49 221 5062-343; Fax +49 221 5062-353; E-mail garridoo@mpipz.mpg.de. Tel: +49 221 5062-350; Fax +49 221 5062-353; E-mail schlef@mpipz.mpg.de.

Introduction

Unlike plants grown under germ-free laboratory conditions, healthy plants in nature live in association and interact with a multitude of microorganisms belonging to several microbial classes, such as bacteria, fungi, oomycetes and protists, collectively known as the plant microbiota (Bulgarelli *et al*., 2013). Marker gene amplicon sequencing has served as an important tool for taxonomic profiling and quantitative surveys of microbial assemblages associated with different plant organs over a range of environmental and experimental conditions, revealing community composition and major factors determining community structure (Hacquard and Schadt, 2015; Thiergart *et al*., 2020). Root-associated bacterial assemblages, assessed by amplicon sequencing of the *16S* rRNA marker gene, are defined by a specific subset of bacteria that originate mainly from the highly diverse soil biota. These communities are characterized by a robust taxonomic pattern at the phylum rank, which comprises the dominant Proteobacteria as well as Actinobacteria, Bacteroidetes and Firmicutes (Bulgarelli *et al*., 2012; Lundberg *et al*., 2012; Hacquard and Schadt, 2015). The main described factors governing differences in root assemblages are, in order of importance,

soil type (edaphic factors such as pH), plant species/genotype and plant age. For leaf-associated bacterial assemblages, the seeding source is less defined because microbiota members can originate from aerosols, insects and soil as well as upward microbial migration from the root (Vorholt, 2012; Müller *et al*., 2016). Root- and leaf-associated microbiota share a similar phylum-level taxonomic composition (Bai *et al*., 2015; Wagner *et al*., 2016). Similar to bacterial communities, plant-associated fungi have been studied at the community level by amplicon sequencing of the internal transcribed spacer (*ITS*) region between the small- and large-subunit rRNA genes or the *18S* rRNA gene (Bazzicalupo *et al*., 2013). Plant-associated fungal assemblages are dominated by members belonging to the Ascomycota and Basidiomycota phyla, with biogeography being the strongest explanatory factor of their variation (Coleman-Derr *et al*. 2016; Thiergart *et al*., 2020; Gao *et al*. 2020).

Systematic establishment of plant-derived microbial culture collections of the plant microbiota has enabled microbiota reconstitution experiments with germ-free plants and taxonomically representative synthetic communities (SynComs), which can be used to address principles underlying community assembly and proposed microbiota functions under defined laboratory environments. This experimental approach has proven critical to the advancement of microbiota research (Bai *et al*., 2015; Lebeis *et al*., 2015; Durán *et al*., 2018; Zhang *et al*., 2019a). For example, more than 400 leaf- and root-derived bacterial strains have been isolated from healthy *A*. *thaliana* grown in natural soil, comprising 35 bacterial families belonging to the aforementioned four phyla (Bai *et al*., 2015). This culture collection represents the majority of bacterial taxa that are detectable by culture-independent *16S* rRNA gene community profiling in the *A*. *thaliana* phyllo- and rhizosphere. Microbiota reconstitution experiments using SynComs from this collection revealed that the bacterial root microbiota provides indirect protection to its host against soil-borne and root-associated harmful fungi, and that this protection is essential for plant survival (Durán *et al*., 2018). Similar reconstitution experiments have shown that bacterial root commensals are necessary for iron nutrition of *A*. *thaliana* in naturally occurring calcareous soils, where poor bioavailability of this soil mineral nutrient limits plant growth (Harbort *et al*., 2020).

Relatively little is known about how the plant microbiota responds to pathogen invasion. The oomycete leaf pathogen *Albugo* has strong effects on epiphytic and endophytic bacterial colonization in *A*. *thaliana*. Specifically, α-diversity (within-sample diversity) decreased and β-diversity (between-sample diversity) stabilized in the presence of *Albugo* infection in leaves, whereas they otherwise varied between plants (Agler *et al*., 2016). The effect of *Alb*. *laibachii* on leaf-associated fungal communities was less consistent and not as clear. Upon foliar defence activation by the downy mildew oomycete pathogen *Hyaloperonospora arabidopsidis*, the host *A*. *thaliana* specifically promotes three bacterial genera in the rhizosphere, namely *Xanthomonas*, *Microbacterium* and *Stenotrophomonas* sp. respectively (Berendsen *et al*., 2018). Although separately these bacteria did not affect the host significantly, together they induced systemic resistance against downy mildew and furthered plant growth.

The analysis of powdery mildew-induced changes in plant leaf microbiota so far rests on field studies with powdery mildew-infected leaf samples (diseased leaves) compared to healthy/less infected leaves in Japanese spindle (*Euonymus japonicus*) (Zhang *et al*., 2019b), pumpkin (*Cucurbita moschata*) (Zhang *et al*., 2018) and English oak (*Quercus robur*) (Jakuschkin *et al*., 2016; reviewed in Panstruga and Kuhn, 2019). In the *E*. *japonicus* study, the authors noticed a reduction in bacterial and fungal diversity in powdery mildew-infected leaves, associated with a general decrease in relative abundance of certain taxa at the genus level (Zhang *et al*., 2019b). Similarly, the richness and diversity of the fungal community were found to be reduced in pumpkin leaves heavily infected by powdery mildew (*Podosphaera* sp.) (Zhang *et al*., 2018). Marked changes in the composition of foliar fungal and bacterial communities were also observed in *Erysiphe alphitoides*-colonized oak (Jakuschkin *et al*., 2016). However, all these studies rely on field samples and natural powdery mildew infections in fluctuating conditions, which complicates deconvolution of microbiota changes caused by variations in environmental factors from those driven by pathogen infection. Moreover, these studies were restricted to the analysis of potential pathogen-induced alterations in the phyllosphere microbiota, while a putative influence of powdery mildew colonization on microbial communities in distal plant tissues/organs such as the root was disregarded.

To test whether powdery mildew infection under controlled conditions impacts local and/or systemic microbial community composition, we examined here the effect of *G*. *orontii* infection on the structure of *A*. *thaliana* leaf and root microbiota in either soil-grown plants or a gnotobiotic plant system pre-treated with defined root- or leaf SynComs. In both settings, we found major powdery mildew-induced shifts in the composition of the local (foliar) assemblages of fungal (natural soil) and bacterial (natural soil and sterile conditions) communities. In the case of

the leaf SynCom, this shift was also associated with a marked increase in bacterial load. Apart from these major changes in the phyllosphere, we also observed a minor systemic effect on the structure of the bacterial root microbiota in conjunction with the leaf SynCom and powdery mildew challenge.

Results

Golovinomyces orontii*-induced changes in root- and leaf-derived natural microbial communities*

Arabidopsis thaliana plants (accession Col-0) were grown in Cologne agricultural soil (CAS) [CAS12; (Bulgarelli *et al*., 2012)] for 6.5 weeks and, subsequently, rosette leaves inoculated with *G. orontii* conidiospores. *Golovinomyces orontii* is a plurivorous powdery mildew species complex with a broad host range, including *A. thaliana* (Kuhn *et al*., 2016; Braun *et al*., 2019). Samples of leaf, root and rhizosphere compartments, as well as unplanted soil, were harvested at 11 days post-incoculation (dpi) at the stage of fungal sporulation, i.e. after completion of the asexual life cycle (Kuhn *et al*., 2016); Fig. 1A and B). Genomic DNA was extracted from these samples and used for PCR-based amplification of the bacterial *16S* rRNA genes and the fungal ribosomal *ITS* regions, *ITS1* and *ITS2*. PCR amplicons were subjected to Illumina sequencing and the resulting sequencing data were used for the analysis of the bacterial and fungal communities in the respective compartments. Information on the number and relative abundance of amplicon sequence variants (ASVs) in each compartment was used to calculate α-diversity (Shannon index; within-sample diversity), β-diversity (Bray–Curtis dissimilarities; between-sample diversity), ASV enrichment and taxonomic composition. Consistent with previous reports (Bulgarelli *et al*., 2012; Schlaeppi *et al*., 2014; Thiergart *et al*., 2020), we found the highest bacterial α-diversity in unplanted soil and the rhizosphere compartment, and lower α-diversity in roots and leaves. In the case of fungi, we noticed an incremental decrease of the Shannon index in soil, roots, the rhizosphere and leaves with both *ITS* primer sets, which was, however, more pronounced in the case of *ITS2*. Compared to bacteria, fungal α-diversity was consistently lower in all compartments analysed (Fig. 1C).

There was no significant difference in bacterial α-diversity between non-inoculated and *G. orontii*-inoculated samples for any of the four compartments analysed (Fig. 1C). By contrast, we observed that in leaves, fungal α-diversity, determined via *ITS1* sequences, was significantly ($P = 0.05$) decreased in *G. orontii*-inoculated leaves (by approximately 70%) but not in any of the other compartments analysed (soil, rhizosphere and root; Fig. 1C). This drop in foliar α-diversity was retained upon *in silico* depletion of *G. orontii* reads, excluding the possibility that the decrease in species richness was due to an overrepresentation of powdery mildew reads (and thus underrepresentation of reads from other fungal taxa) in the samples. A similar outcome was obtained with *ITS2* amplicons (Fig. 1C). Together, these findings suggest that *G. orontii* leaf colonization reduced the diversity of leaf-associated fungal communities, whereas α-diversity of fungal communities in other compartments and bacterial assemblages remained unaltered.

Analysis of β-diversity using principal-coordinates analysis (PCoA) of Bray–Curtis dissimilarities revealed distinctive bacterial community compositions in unplanted soil, rhizosphere, root and leaf compartments (Fig. 2A). We noted that β-diversity of leaf-associated bacterial assemblages changed in response to *G. orontii* inoculation, whereas bacterial communities remained indistinguishable in the other compartments ($P = 0.029$; Fig. 2C and F). This suggests that *G. orontii* exerts a local effect on bacterial community profiles but not systemically on the bacterial root and/or rhizosphere microbiota. Closer inspection of the *G. orontii*-induced bacterial community shifts in leaves revealed a broad range of bacterial ASVs that showed significantly altered relative abundances (differentially abundant ASVs; $P < 0.05$; Supplementary Fig. 1). This shift affected ASVs that are enriched or depleted (4.4% and 2.5% of differentially abundant ASVs respectively). The majority of taxa with differential fold changes were either undetectable in the absence of *G. orontii* (enriched taxa) or undetectable following *G. orontii* challenge (depleted taxa; Supplementary Fig. 1). Similar to the leaf-associated bacterial commensals, analysis of β-diversity of the leaf-associated fungal community revealed a marked shift following *G. orontii* inoculation (Fig. 2B; *ITS1* Fig. 2D; *ITS2* Fig. 2E). No alteration of fungal community composition could be found in the case of soil, rhizosphere and roots, apart from a weakly significant change in the case of ITS2/rhizosphere combination (Fig. 2F). As with the changes in α-diversity (Fig. 1C), the differentiation in distinct leaf-associated fungal communities following powdery mildew infection was not due to an overrepresentation of *G. orontii* reads, as indicated by a similar outcome upon *in silico* depletion of the corresponding reads (Fig. 2F).

Permutational multivariate analysis of variance revealed that *G. orontii* leaf colonization explained approximately 15% and 34%–45% (*ITS1* and *ITS2*) of the variation of the leaf-associated bacterial or fungal communities respectively (Fig. 2F). To explore the changes driving this variation in community structure, we calculated the proportion of bacterial ASVs with differential

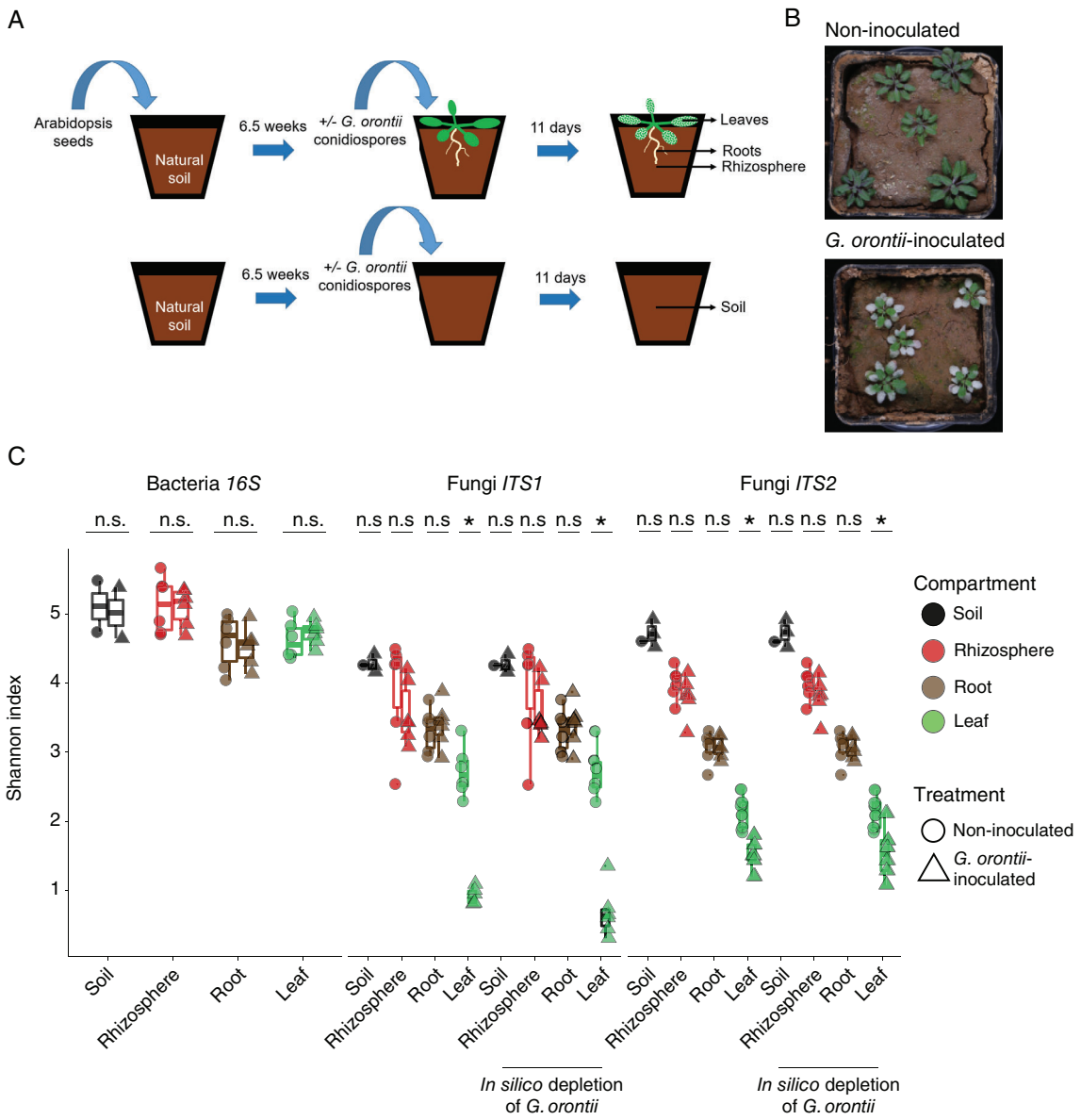

Fig. 1. *Golovinomyces orontii* infection reduces leaf fungal α-diversity in plants grown in natural soil.
A. Scheme illustrating the setup of the natural soil experiment.
B. Representative photographs of non-inoculated and *G. orontii*-inoculated plants grown in natural soil.
C. Box plots of within-sample diversity (Shannon index) for each compartment and condition. Significant differences in microbial community diversity within compartments are marked with an asterisk (Student's *t*-test, $^*P < 0.05$; n.s., not significant).

abundance upon *G. orontii* infection at the order level. For the majority of bacterial orders with multiple differentially abundant ASVs, both enriched and depleted ASVs were found, although we observed more differentially enriched than differentially depleted ASVs. The two orders with the greatest proportion of differentially abundant ASVs were Burkholderiales and Rhizobiales (approximately 33% and 9.5% respectively; Fig. 3A), two abundant bacterial taxa robustly present in *A. thaliana* leaf microbiota (Garrido-Oter *et al*., 2018). We also tested whether differentially enriched or depleted ASVs for a given bacterial order affect its aggregated relative abundance. Although the aggregated relative abundance of Burkholderiales, Flavobacteriales and Rhizobiales increased, the aggregated relative abundance of Pseudonocardiales was reduced upon *G. orontii* inoculation ($P < 0.05$; Fig. 3B). As these four bacterial orders belong to three phyla, Proteobacteria, Actinobacteria and Bacteroidetes, *G. orontii* colonization influenced the abundance of phylogenetically distantly related bacterial leaf commensals.

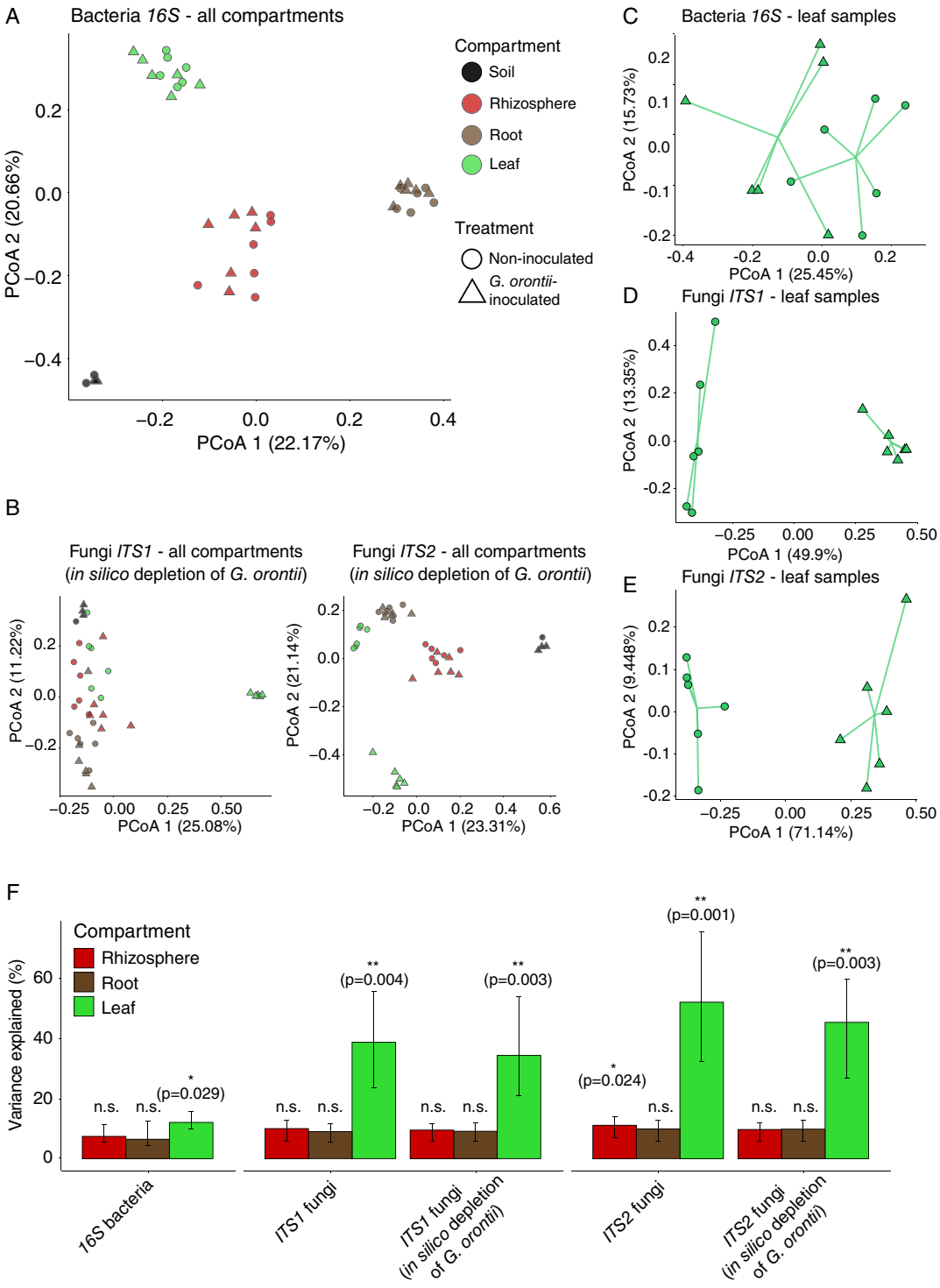

Fig. 2. *Golovinomyces orontii* colonization induces changes in local bacterial and fungal communities.
A. PCoA plot of Bray–Curtis dissimilarities between bacterial community samples, colour-coded by compartment and shaped based on treatment.
B. PCoA plot of Bray–Curtis dissimilarities between fungal community samples for *ITS1* (left) and *ITS2* (right) amplicons following *in silico* depletion of *G. orontii* reads, colour-coded by compartment and shaped based on treatment.
C. Subset of leaf samples where separation between treatments (non-inoculated vs. *G. orontii*-inoculated) can be observed.
D–E. PCoA plots of fungal communities in leaf samples for *ITS1* (D) and *ITS2* (E) profiles.
F. Explained variance of bacterial and fungal community structures upon *G. orontii* infection, colour-coded by compartment. Note that for fungal communities, data without and with *in silico* depletion of *G. orontii*-assigned reads are shown. *$0.01 \geq P < 0.05$, **$0.001 \geq P < 0.01$.

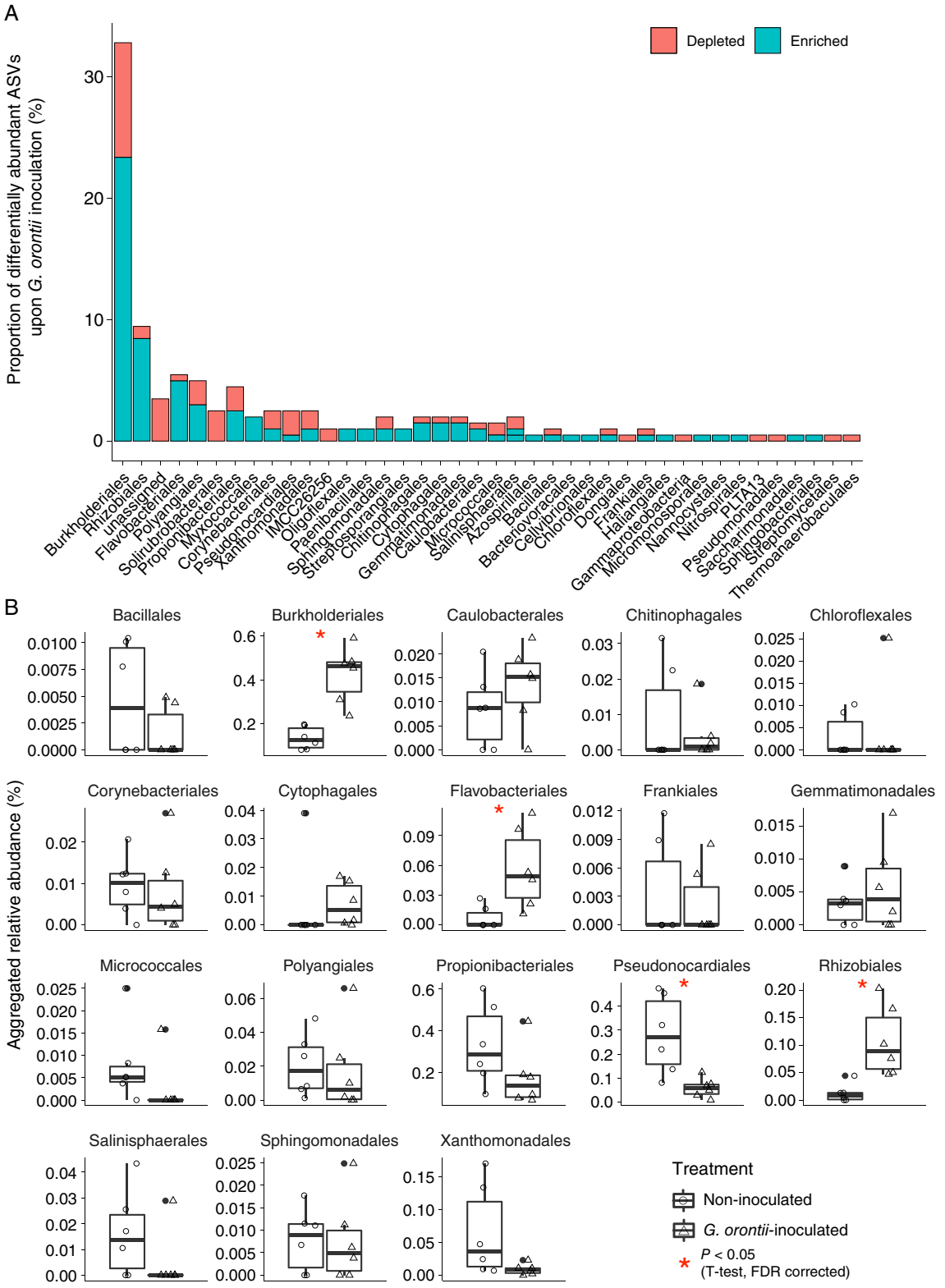

Fig. 3. *Golovinomyces orontii* infection leads to both enrichment and depletion in relative abundances of leaf bacterial ASVs.
A. Proportion of ASVs that significantly changed their relative abundance upon infection with *G. orontii*, grouped by order level, in relation to the overall number of ASVs affected.
B. Log-transformed aggregated relative abundance of each bacterial order shown in (A), which has both enriched and depleted ASVs, compared between non-inoculated and *G. orontii*-inoculated conditions.

Closer inspection of the *G. orontii*-induced fungal community shift showed that a great proportion (15%–34%) of taxa were depleted (Supplementary Figs 2 and 3), including abundant and low abundant members of a variety of fungal classes. This result is consistent with the aforementioned *G. orontii*-induced reduction in fungal α-diversity (Fig. 1C). However, nine fungal taxa were significantly enriched, with members of the Erysiphales and the Golubeviales showing the highest fold change. Besides *G. orontii*, we noticed the presence of other powdery mildew species (*Erysiphe* spp.) among the enriched fungal taxa. These could either be contaminations in our inoculum or species introduced from the environment in the course of the experiment 'hitchhiking' on the diseased plants.

In summary, we observed a major shift in the resident fungal community in *G. orontii*-infected leaves of plants grown in natural soil, characterized by predominantly depleted taxa compared to non-infected plants. In contrast, changes in the leaf-associated bacterial communities were more limited, with both enriched and depleted taxa. No alterations were seen in the systemic root tissue.

Golovinomyces orontii-*induced changes in root- and leaf bacterial SynComs*

Next, we tested whether and to which extent we could recapitulate results obtained with plants grown in natural soil using a system of reduced microbial complexity. To this end, we examined the impact of *G. orontii* leaf infection using a gnotobiotic *A. thaliana* system and defined *A. thaliana* root and leaf bacterial consortia (root- and leaf-derived *At*-SPHERE strains), which comprise representatives of the majority of taxa that are detectable by culture-independent *16S* rRNA amplicon sequencing in association with plants grown in natural soil (Bai *et al*., 2015). In this gnotobiotic plant system, *A. thaliana* surface-sterilized seeds were sown on a calcined clay matrix. In a first experiment, we inoculated prior to sowing a defined bacterial consortium consisting of 88 root-derived bacterial commensals (designated here 'root SynCom'), co-cultivated the consortium with the host for 4.5 weeks, followed by either *G. orontii* conidiospore inoculation or no inoculation. At 11 dpi, leaf, matrix and root samples were harvested and the corresponding DNA preparations were subjected to *16S* rRNA amplicon sequencing (Fig. 4A and B). PCoA of Bray–Curtis dissimilarities of the bacterial consortia revealed their separation according to compartment (Fig. 4C and D). In addition, in the case of the root-derived SynCom, root-associated consortia were found to be more similar to matrix-associated communities, while still separated from the leaf-resident assemblages (Fig. 4C; Supplementary Fig. 4), indicating differential colonization of above- and below-ground plant organs by members of the root-derived SynCom. The leaf-resident community was probably the result of upward bacterial migration from roots to shoots during co-cultivation. In contrast to matrix and root samples, which showed no separation following pathogen challenge (Fig. 4C), leaf samples collected from matrix-inoculated root SynComs differentiated significantly upon *G. orontii* infection ($P = 0.02$; Fig. 4E and H, Supplementary Fig. 4). This pattern is reminiscent of the *G. orontii*-induced impact on *A. thaliana* plants grown in natural soil with an infection-induced change in the bacterial leaf microbiota but non-responsiveness of the root-associated community (cf. Figure 2F and Fig. 4H).

In a second experiment, *A. thaliana* plants were grown on a sterilized calcined clay matrix and, at the age of 3.5 weeks, leaves were spray-inoculated with a defined bacterial consortium consisting of 103 leaf-derived bacterial commensals (designated here 'leaf SynCom'). Fourteen days after plant-bacteria co-cultivation, leaves were either inoculated with *G. orontii* conidiospores or left non-inoculated. At 7 dpi, leaf and root samples were collected and the corresponding microbial DNA preparations were subjected to *16S* rRNA gene amplicon sequencing (Fig. 4A and B). PCoA of Bray–Curtis dissimilarities of the bacterial consortia show their separation according to compartments (Fig. 4D and Supplementary Fig. 5). Closer inspection revealed a significant separation of non-inoculated and *G. orontii*-inoculated samples in both roots and leaves ($P = 0.012$ and $P = 0.002$ respectively; Fig. 4F–H). The *G. orontii*-induced shift in the leaf-associated bacterial consortium is consistent with the shift of the leaf microbiota observed in *G. orontii*-inoculated plants in natural soil (cf. Figs 2F and 4H). However, unlike the absence of a systemic effect on the bacterial root microbiota in natural soil upon leaf powdery mildew infection (Fig. 2F), the in part possibly ectopically located leaf SynCom commensals on roots were responsive to *G. orontii* infection in the gnotobiotic plant system (Fig. 4G and H; see Discussion).

To assess potential changes in absolute abundance of leaf-associated bacterial communities following *G. orontii* infection, we performed qPCR of the corresponding leaf samples with PCR primers specific for bacterial *16S* rRNA and a *G. orontii*-specific gene, and normalized against an *A. thaliana*-specific amplicon (see Experimental procedures). Unexpectedly, we found a twofold increase in bacterial load in *G. orontii*-colonized leaf samples, whereas *G. orontii* biomass on leaves in either the presence or absence of the bacterial SynCom remained unaltered (Fig. 5A). The increase in bacterial load in *G. orontii*-inoculated leaves could be seen across multiple taxonomic classes, most prominently in Actinobacteria, Alphaproteobacteria and Flavobacteria (Fig. 5B and Supplementary Fig. 6).

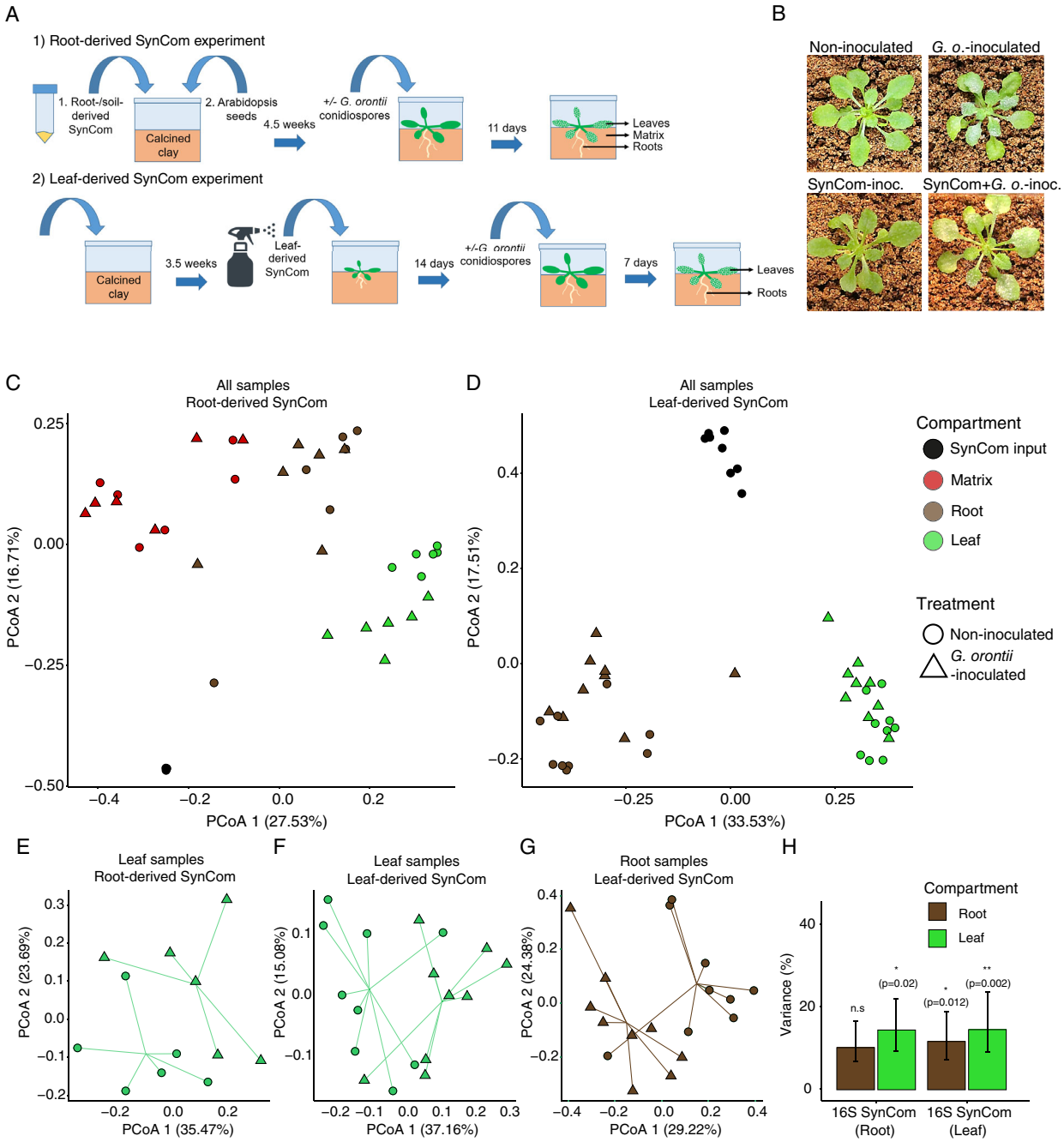

Fig. 4. *Golovinomyces orontii* infection induces changes mainly in local bacterial SynComs.
A. Scheme illustrating the set-up of the two SynCom experiments.
B. Representative photographs of non-inoculated and *G. orontii*-inoculated plants, with and without prior inoculation with the leaf-derived SynCom. Note that the slight leaf yellowing is a symptom of the SynCom treatment.
C. PCoA of Bray–Curtis distances of all compartments inoculated with Root *At*-SPHERE strains.
D. PCoA of Bray–Curtis distances of all compartments inoculated with Leaf *At*-SPHERE strains.
E–G. Subset of leaf (E and F) and root samples (G), inoculated with either Root *At*-SPHERE strains (E) or Leaf *At*-SPHERE strains (F and G), showing the effect on bacterial community structure upon *G. orontii* infection (different shapes).
H. Explained variance on bacterial community structure upon *G. orontii* infection (PERMANOVA analysis on Bray–Curtis dissimilarities). *0.01 ≥ P < 0.05, **0.001 ≥ P < 0.01.

We finally took advantage of the *G. orontii*-infected plants in the gnotobiotic system to analyse the composition of our fungal inoculum. Although *G. orontii*, as expected, is the predominant taxum of the inoculum, this revealed the presence of additional fungal genera of marked abundance, including some that contain known

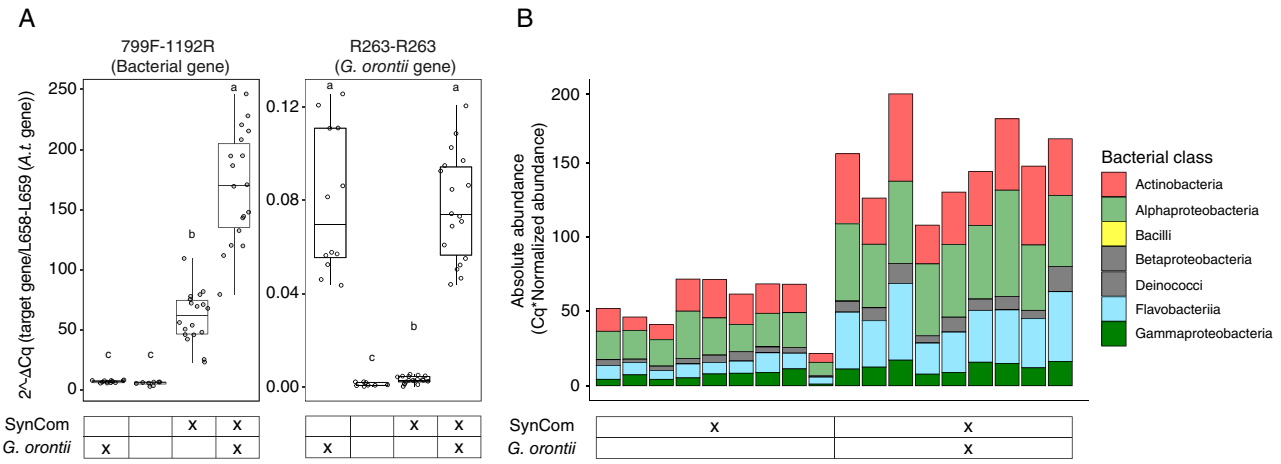

Fig. 5. *Golovinomyces orontii* colonization increases leaf bacterial load.
A. Bacterial (left panel) and *G. orontii* (right panel) load calculated by the quantification of the bacterial *16S* rRNA gene and a *G. orontii*-specific gene relative to an *A. thaliana* reference gene.
B. Absolute abundance of each strain utilized in this experiment, colour-coded by their taxonomic assignment at the family level, in leaf SynCom-inoculated leaves that were either non-inoculated or inoculated with *G. orontii*.

hyperparasites of powdery mildews (*Acremonium* sp. and *Golubevia* sp.) and another powdery mildew genus (*Erysiphe* sp., >6% average aggregated relative abundance; Supplementary Fig. 7). Furthermore, we checked the proportion of reads in the SynCom amplicon raw data that could not be successfully aligned to SynCom reference sequences between non-inoculated and *G. orontii*-inoculated samples. This resulted in an average proportion of only 10% (9%–11%) of unaligned reads in both conditions (non-inoculated- and *G. orontii*-inoculated leaf samples), making it unlikely that our SynCom and natural soil-based community data are affected by bacterial contamination of the fungal inoculum.

Discussion

In this study, we analysed the influence of laboratory-propagated powdery mildew (*G. orontii*) inoculum on leaf- and root-associated natural and synthetic microbial communities in controlled environments, in *A. thaliana* (Figs 1A and 4A). For the experiments conducted in natural soil (Fig. 1A and B), we observed no alteration in bacterial α-diversity in all tested compartments (soil, rhizosphere, root and leaf) following powdery mildew challenge, while α-diversity of the foliar fungal community was strongly reduced (Fig. 1C). The more pronounced effect seen with the *ITS1* primers compared to the *ITS2* primer pair was probably a consequence of a greater molecular diversity recovered with the former primers (Bazzicalupo *et al*., 2013). The substantial reduction in α-diversity of the leaf-associated fungal community upon powdery mildew infection is an indication that the invasive pathogen outcompetes many resident fungal leaf endophytes (15%–31% of ASVs), for example due to a powdery mildew pathogen-induced shift in sink–source relationships in infected compared to pathogen-free leaves. During a compatible powdery mildew interaction, photosynthetic activity of the plant host is progressively reduced both in cells directly below fungal colonies and in adjacent cells, and this process is associated with an increase in apoplastic invertase activity and an accumulation of hexoses thought to favour pathogen nutrition (Wright *et al*., 1995; Swarbrick *et al*., 2006; Eichmann and Hückelhoven, 2008). Alternative explanations may include fungus-specific antibiosis by *G. orontii* or activation of plant immune responses by the fungal invader or its associated microbial contaminants. The former explanation appears unlikely because the obligate biotrophic pathogen has an unusually low genomic capacity for the biosynthesis of specialized metabolites (Spanu *et al*., 2010). *Golovinomyces orontii* pathogenesis stimulates the accumulation of the defence hormone salicylic acid (SA) at later stages of infection (4 dpi) in leaves, and SA-dependent defence signalling limits hyphal growth and pathogen reproduction (Dewdney *et al*., 2000; Stein *et al*., 2008; Poraty-Gavra *et al*., 2013). For this reason, we consider it plausible that the dramatic reduction in α-diversity of the resident community of asymptomatic leaf-associated fungi in response to *G. orontii* invasion is linked to pathogen-induced and SA-dependent immune responses and/or changes in metabolic sink–source relationships. In a recent wheat study, the impact of the hemibiotrophic fungal pathogen *Zymoseptoria tritici* on bacterial community structure was studied in both pathogen-inoculated and adjacent pathogen-free leaves. Bacterial species richness and community composition were strongly altered in both *Z. tritici*-inoculated and

pathogen-free leaves of a resistant but not a susceptible wheat cultivar at 4 dpi. The authors concluded that this outcome could be due to a systemic immune response with upregulated immune-related metabolites in pathogen-free leaves of the resistant cultivar (Seybold *et al*., 2020). As an alternative scenario, we can, however, not rule out that powdery mildew pathogens deploy secreted effector proteins to antagonize resident endophytic fungi that compete for the same ecological niche (Snelders *et al*., 2018). For example, two effector proteins of the fungal phytopathogen *Verticillium dahliae* exert antimicrobial activity. This soil-borne pathogen deploys effector proteins not only to facilitate host colonization but also to modulate microbiota composition inside the host and in the soil environment (Snelders *et al*., 2020). Potentially different metabolic demands of leaf-associated commensal bacteria compared to fungi together with the ASV-level compensatory changes seen within numerous bacterial orders of the leaf microbiota could explain why the *G*. *orontii*-induced shift in nutrient availability and immune status does not affect bacterial commensal diversity in the same way.

Consistent with a strong decrease in fungal species richness on *G*. *orontii*-infected leaves of plants grown in natural soil, we found that the altered fungal community profile is characterized by a reduction in relative abundances for most and an increase in relative abundances of a few taxa, while the local bacterial community profile was only slightly affected (Fig. 2; Supplementary Fig. 2 and 3). Fungal endophytes whose relative abundance increased upon *G*. *orontii* infection comprised mainly one other powdery mildew species (*Erysiphe* sp.), or fungi typically associated with them, such as *Acremonium* sp. and *Golubevia* sp., which are hyperparasites of powdery mildew pathogens (Malathrakis, 1985; Russ *et al*., 2021). Given that the latter two genera are already present in our *G*. *orontii* inoculum (Supplementary Fig. 7), the observed increase in their relative abundance upon plant infection is most likely a direct consequence of their association with *G*. *orontii* and not because of a powdery mildew-triggered increase in the relative abundance of leaf-resident fungi.

Closer inspection of the *G*. *orontii*-induced shift of bacterial community diversity in leaves revealed 40 bacterial orders, containing several ASVs whose relative abundance was depleted or enriched (Fig. 3A and Supplementary Fig. 1). However, significant alterations in aggregated ASV-level relative abundances were seen only in four bacterial orders, with three of them showing an increase and one a decrease (Burkholderiales, Flavobacteriales, Rhizobiales and Pseudonocardiales respectively; Fig. 3B). This pattern suggests widespread compensatory changes at the ASV level within bacterial orders that may allow maintenance of the higher taxonomic structure of the bacterial leaf microbiota during powdery mildew pathogenesis. The fungal pathogen thus mediates local community shifts in the aggregated relative abundances limited to four bacterial orders belonging to the three main phyla of the *A*. *thaliana* microbiota (Actinobacteria, Proteobacteria and Bacteroidetes; (Bulgarelli *et al*., 2012). In addition, in our SynCom experiments, colonization by the biotrophic pathogen unexpectedly increased the load of bacterial commensals in leaves by twofold, and this increase was seen roughly equally proportional for all bacterial classes analysed (Fig. 5). The rise in bacterial numbers could be an indirect consequence of the altered sink–source relationships upon infection with the biotrophic pathogen, which turns infected leaves into a metabolic sink associated with an altered availability of non-structural carbohydrates (Wright *et al*., 1995; Swarbrick *et al*., 2006). Consequently, the bacterial commensals might benefit from an accumulation and/or alteration in fluxes of apoplastic hexose sugars and reduction in export of sucrose from the leaf.

In the case of bacteria, changes were only detectable locally (in the infected leaves) but not systemically (in roots or rhizosphere compartments) and only applied to community diversity, while species richness remained unaltered (Figs 1C and 2). The subtle shift in local (foliar) bacterial diversity could be an indirect consequence of the significant alterations in fungal community richness and diversity upon *G*. *orontii* invasion. However, at the bacterial order level, we noted a striking overall similarity of the *G*. *orontii*-induced local bacterial community shifts between the natural soil and bacterial SynCom experiments (significant increases in the relative abundance of Burkholderiales, Flavobacteriales and Rhizobiales and a similar trend for Caulobacterales; Supplementary Fig. 6B). This suggests that our gnotobiotic plant system recapitulates features of the powdery mildew pathogen-induced bacterial community shifts seen in plants grown in natural soil. It further rules out the possibility that these shifts are the result of bacterial immigration into vacated leaf niches that had to be abandoned by the resident fungal endophytes in the course of *G*. *orontii* pathogenesis.

The only systemic effect on root-associated microbes upon powdery mildew infection reported so far involves nitrogen-fixing rhizobia, which engage in root symbiosis with legumes. In pea (*Pisum sativum*), powdery mildew (*Erysiphe pisi*) colonization was found to result in both a reduction of nodulation and reduced size of root nodules in the leaf-infected plants (Singh and Mishra, 1992). The absence of a systemic effect on the bacterial root microbiota following *G*. *orontii* challenge differs from *A*. *thaliana* plants infected with the foliar downy mildew pathogen, the obligate biotrophic oomycete *H*. *arabidopsidis*. Colonization of leaves with *H*. *arabidopsidis* promoted the specific enrichment of three bacterial taxa (*Xanthomonas*, *Stenotrophomonas* and *Microbacterium* spp.) from soil to

the rhizosphere, where these three taxa synergistically induce systemic defence responses and further plant growth, resulting in enhanced disease resistance against downy mildew (Berendsen *et al*., 2018). Although *G. orontii* and *H. arabidopsidis* are both obligate biotrophic foliar pathogens, only the latter pathogen can infect leaf mesophyll cells and ramify inside this organ, and this may be one reason why only *H. arabidopsidis* can systemically induce changes in the bacterial root microbiota.

Our experiments using germ-free plants, pre-inoculated with a leaf-SynCom and either left non-inoculated or challenged with *G. orontii* (Fig. 4), recapitulated in parts the pathogen-induced shift in bacterial community profiles of plants grown in natural soil (Supplementary Fig. 6B). However, in these experiments also the root samples showed a significant difference in β-diversity of the bacterial root microbiota following *G. orontii* inoculation (Fig. 4G and H). As roots were not pre-inoculated in this experiment, the bacteria recovered from root samples must have originated from the leaf inoculation and either reached the below-ground roots in calcined clay accidentally (e.g. by wash-off) or by downward migration, for example via the plant vasculature. Irrespective of the mechanism(s) underlying the in part possibly ectopic root colonization of the leaf-inoculated bacterial SynCom, this result indicates a (subtle) systemic effect of foliar inoculation with the powdery mildew pathogen on the root-associated bacterial community, which was not seen in the experiment with plants grown in natural soil (see above and Fig. 2B). This disparity is probably the result of different conditions in the two experimental setups. The SynCom experiment involves a reduced complexity of the bacterial community, allowing us to track the relative abundance of many members with strain-specific resolution rather than the relative abundance of ASVs, which could represent an average of multiple genetically polymorphic strains that share an identical *16S* rRNA sequence. Therefore, the higher complexity of the root microbiota in natural soil may mask putative systemic effects on bacterial assemblages induced by *G. orontii* colonization. Alternatively, or in addition, the absence of an authentic soil bacterial inoculum may prevent proper priming of plant immunity prior to powdery mildew leaf inoculation, resulting in a stronger systemic effect.

It is surprising that the pre-inoculated leaf SynCom did not mediate detectable protective activity against the fungal powdery mildew pathogen, e.g. through activation of defence-associated gene expression in leaves or antagonistic bacteria–fungus interactions, as demonstrated by a similar *G. orontii* biomass in the presence or absence of the leaf-derived SynCom (Fig. 5A; (Vogel *et al*., 2016; Durán *et al*., 2018). In roots, the presence of the bacterial microbiota is essential for indirect protection and survival of *A. thaliana* against the otherwise detrimental activity of diverse fungal root endophytes (Durán *et al*., 2018). In *A. thaliana* leaves, several members of the genus *Sphingomonas*, originally isolated from plants, conferred plant protection against the foliar bacterial pathogen *P. syringae* DC3000 and *Xanthomonas campestris* in a gnotobiotic system, whereas no protection was observed by colonization with members of the genus *Methylobacterium* (Innerebner *et al*., 2011). Thus, our results suggest that the bulk of the resident bacterial leaf microbiota of *A. thaliana* does not have a dedicated role in indirect protection against epiphytic *G. orontii* invasion in the tested gnotobiotic system. Whether this is also true for fungal leaf pathogens that colonize mesophyll cells in the leaf interior remains to be seen.

Part of the powdery mildew-induced changes in the *A. thaliana* microbiota could be due to the suppression of plant immunity and reprogramming of host cells for parasitism by the obligate biotrophic pathogen (Schulze-Lefert and Panstruga, 2003). The effect of defence suppression in colonized and neighbouring leaf epidermal cells is, for example, evident by the phenomenon of 'induced accessibility', which refers to enabled host cell entry of non-adapted powdery mildews in the vicinity of established powdery mildew infection sites (Yamaoka *et al*., 1994; Lyngkjær and Carver, 1999a; Lyngkjær and Carver, 1999b; Lyngkjær *et al*., 2001). Powdery mildew-induced alterations of the host transcriptome likely represent the net outcome of counteracting activities of the plant immune system and the fungal intruder (Fabro *et al*., 2008). Although leaf-associated bacterial commensals also extensively reprogram host transcriptomes, stimulating and/or repressing the activity of gene clusters enriched in immunity-and metabolism-associated functions in leaves (Vogel *et al*., 2016), the additional pathogen-specific changes in the host transcriptional profile during infection likely contribute to modulating the quantity and composition of the resident microbiota.

Based on the analysis of our laboratory-generated *G. orontii* inoculum on gnotobiotic plants, we noted that approximately 50% of the reads originate from different fungi, including at least two powdery mildew hyperparasites and another powdery mildew species (*Erysiphe* sp.; Supplementary Fig. 7). By contrast, according to our data, bacterial contamination of the inoculum appears to be negligible. Our findings highlight the difficulties of maintaining a plant pathogen with an obligate biotrophic lifestyle that must be propagated on living host plants in pure culture. The co-occurrence with these microbes may balance powdery mildew proliferation. These observations might have implications not only for the interpretation of aspects of the data obtained in this work but

also for studies that use other obligate biotrophic plant pathogens.

Experimental procedures

Plant material

Arabidopsis thaliana Col-0 wild-type (Arabidopsis stock center accession N60000) was used as a model plant system. Seeds were surface-sterilized by treating them with 70% ethanol for 20 min and drying them under a sterile hood. Subsequently, the seeds were stratified overnight at 4°C.

Microbial strains

The *At*-SPHERE bacterial strains used in this study have been previously reported (Bai *et al*., 2015) and are summarized in Supplementary Table 1. *Golovinomyces orontii* (isolate MPIPZ) was used as a powdery mildew infection agent. *Golovinomyces orontii* was regularly propagated every week on 4- to 5-week-old super-susceptible *A. thaliana eds1* plants. Powdery mildew inoculation was conducted by leaf-to-leaf contact of healthy plants with rosette leaves of heavily infected *eds1* plants, as reported previously (Acevedo-Garcia *et al*., 2017).

Natural soil experiment

Arabidopsis thaliana Col-0 seeds were sown into 7 × 7 greenhouse pots filled with CAS batch 12 and grown under short-day greenhouse conditions for 6.5 weeks (12 pots containing five seeds each). Then, plants in half of the pots ($n = 6$) were inoculated with *G. orontii* while the plants in the other pots ($n = 6$) remained non-inoculated, and all pots were transferred to a growth chamber (day: 21°C, 10 h light; night: 19°C; 70% humidity). Four pots with unplanted soil ($n = 2$ non-inoculated, $n = 2$ inoculated) served as additional controls. At 11 dpi, bulk soil, rhizosphere, root and leaf samples were harvested, as previously described [Fig. 1A; (Bulgarelli *et al*., 2012; Bai *et al*., 2015)]. Rhizosphere, root and leaf samples were pooled from the five plants per pot, resulting in $n = 6$ samples for subsequent microbial profiling.

SynCom experiments in gnotobiotic system

Calcined clay was washed several times with tap water followed by MiliQ water. After removal of the liquid, the calcined clay was autoclaved following a liquid cycle (121°C, 20 min), and oven-dried at 60°C for 4 weeks. Of the washed, autoclaved and dried calcined clay, 100 g were transferred into a previously sterilized Magenta GA-7 plant culture box (Thermo Fisher Scientific, Schwerte, Germany), sealed and autoclaved again, and dried overnight prior to the experiment.

The bacterial strains used were pre-grown for 7 days in tryptic soy broth 50% (TSB 50%, Sigma-Aldrich), and washed with 10 mM $MgCl_2$ (series of centrifugations and removal of supernatant, and final resuspension in $MgCl_2$) to remove any byproducts from the bacterial cultures. A total of 88 and 103 bacterial strains were selected, which represent a wide taxonomic range and that are differentiable based on their *16S* rRNA gene sequence (see Table S1), for the root and leaf SynComs respectively, and mixed in three separate inputs. For each of the three bacterial mixes, the OD_{600} was set to 0.5 (root SynCom) and to 0.2 (leaf SynCom) with 10 mM $MgCl_2$. A sample of each of the bacterial inputs was taken as a reference for bacterial community composition.

For the root-derived SynCom experiment, 70 ml ½ MS medium (including vitamins without sucrose, pH 7, Sigma-Aldrich GmbH, Cat No. M5524-1L, Taufkirchen, Germany) was mixed with 1 ml of the SynCom culture and used to inoculate one calcined-clay-containing Magenta box ($n = 12$). As a control, to a separate batch of magenta boxes only ½ MS medium without SynCom culture was added ($n = 12$). Surface-sterilized *A. thaliana* Col-0 seeds were sown at the four corners of the boxes and the lids were closed. Plants were grown in a growth cabinet under short-day conditions (day: 22°C, 10 h light; 70% humidity) for 4.5 weeks. Then, plants were inoculated with *G. orontii* under sterile conditions [$n = 6$, no SynCom culture (½ MS medium only, mock treatment), and $n = 6$, previously treated with SynCom culture]. A set of boxes that were either mock- ($n = 6$) or SynCom-inoculated ($n = 6$) were opened, but not inoculated with *G. orontii*, serving as a control. At 11 dpi, root and leaf tissues were harvested (Fig. 4A). In addition, SynCom input samples ($n = 3$) were subjected to microbial profiling.

For the leaf-derived SynCom experiment, 70 ml ½ MS media (including vitamins without sucrose, pH 7, Sigma-Aldrich GmbH, Cat No. M5524-1L) was mixed into the calcined-clay-containing magenta boxes, and surface-sterilized *A. thaliana* seeds were sown at the four corners of the boxes. Plants were grown in a growth cabinet under short-day conditions (day: 21°C, 10 h light; night: 19°C; 70% humidity) for 3.5 weeks. Then, a 10-fold dilution of the leaf SynCom in 10 mM $MgCl_2$ was sprayed five times with a Reagent Sprayer (CAMAG®Glass Reagent Spray, Muttenz, Switzerland) onto the *A. thaliana* plants (see (Bai *et al*., 2015); here: 1 spray volume = approximately 35 µl; $n = 18$). At 14 days after the addition of the SynCom or respective mock (10 mM $MgCl_2$) treatments, plants were inoculated with *G. orontii* under sterile conditions ($n = 6$, no SynCom, and $n = 9$,

previously treated with SynCom culture). A set of boxes that were either mock- ($n = 9$) or SynCom-inoculated ($n = 9$) were opened, but not inoculated with *G. orontii*, serving as a control. At 7 dpi, root and leaf tissues were harvested (Fig. 4A). In addition, SynCom input samples ($n = 8$) were subjected to analysis.

Microbial profiling from plant tissues

Total DNA was extracted from all samples mentioned above using the FastDNA SPIN Kit for Soil (MP Biomedicals, Solon, USA). Samples were homogenized in Lysis Matrix E tubes (MP Biomedicals, Heidelberg, Germany) using the Precellys 24 tissue lyzer (Bertin Technologies, Montigny-le-Bretonneux, France) at 6200 rpm for 30 s. DNA samples were then eluted in 80 μl nuclease-free water and used for bacterial and fungal community profiling (Durán *et al*., 2018). Concentrations of DNA samples were fluorescently quantified, adjusted to 3.5 ng μl^{-1}, and samples were used as templates in a two-step PCR amplification protocol. In the first step, the V5–V7 region of bacterial *16S* rRNA (primers 799F-1192R), fungal *ITS1* (primers ITS1F-ITS2) and *ITS2* (primers fITS7-ITS4) regions were amplified. Under a sterile hood, each sample was amplified in triplicate in a 25 μl reaction volume containing 2 U DFS-*Taq* DNA polymerase, 1× incomplete buffer (both Bioron GmbH, Ludwigshafen, Germany), 2 mM $MgCl_2$, 0.3% BSA, 0.2 mM dNTPs (Life Technologies GmbH, Darmstadt, Germany) and 0.3 μM forward and reverse primers. PCR was performed using the same parameters for all primer pairs (94°C/2 min, 94°C/30 s, 55°C/30 s, 72°C/30 s, 72°C/10 min for 25 cycles). Afterwards, single-stranded DNA and proteins were digested by adding 1 μl of Antarctic phosphatase, 1 μl exonuclease I and 2.44 μl Antarctic Phosphatase buffer (New England BioLabs GmbH, Frankfurt, Germany) to 20 μl of the pooled PCR product. Samples were incubated at 37°C for 30 min and, subsequently, enzymes were deactivated at 85°C for 15 min. Samples were then centrifuged for 10 min at 4000 rpm, and 3 μl of this reaction was used for a second PCR, prepared in the same way as described above, using the same amplification protocol but with the number of cycles reduced to 10, and with primers including barcodes with Illumina adaptors (Table S1). PCR product quality was controlled by loading 5 μl of each reaction on an agarose gel and affirming that no band was detected in the negative control without template DNA. Afterwards, the replicated reactions were combined and purified as follows: bacterial amplicons were loaded on a 1.5% agarose gel and run for 2 h at 80 V; bands with the correct size of ~500 bp were cut out and purified using the QIAquick gel extraction kit (QIAGEN GmbH, Hilden, Germany). Fungal amplicons were purified using Agencourt AMPure XP beads (Thermo Fisher Scientific). DNA concentration was again fluorescently determined, and 30 ng DNA of each of the barcoded amplicons were pooled in one library per microbial group. Each library was then purified and reconcentrated twice with Agencourt AMPure XP beads, and 100 ng of each library was pooled together. Paired-end Illumina sequencing was performed in-house using the MiSeq sequencer and custom sequencing primers (Supplementary Table 1). Numbers of samples per compartment and condition (natural soil and SynCom experiments), as well as the number of detected ASVs per compartment and condition (natural soil experiment), are given in Supplementary Table 1. Note that commonalities of operational taxonomic units derived from *ITS1* and *ITS2* amplicons are generally low (Yang *et al*., 2018). We, therefore, examined the correlation between our *ITS1*- and *ITS2*-derived taxonomic profiles at the order level (after *in silico* subtraction of *G. orontii*-associated reads) and found that these are correlated well, except for those found in only one of the profiles (Pearson's correlation coefficient = 0.996, $P < 2.2e\text{-}16$).

Absolute quantification of microbial load in plant tissues

Genomic DNA from leaves inoculated with SynCom alone ($n = 9$), *G. orontii* alone ($n = 6$), both SynCom and *G. orontii* ($n = 9$), or mock-treated ($n = 4$) was used for absolute quantification of microbial load. Genomic DNA was fluorescently quantified and diluted to an equal concentration of 4 ng/μl. Each sample was subsequently used for absolute quantification via PCR (qPCR) by adding SYBR green to monitor the PCR amplification in real-time. Each sample was amplified in duplicate: 4 μl of template was mixed with 7.5 μl of SYBR green (brand), together with 1.2 μl of forward primer and 1.2 μl of reverse primer, to a final volume of 15 μl of reaction. For each organism, a specific primer pair was selected: for bacterial assessment, the *16S* rRNA gene [primers 799F-1192R, (Wippel *et al*., 2021)]; for *G. orontii*, a GDSL lipase-like gene (primers R263-R264, (Weßling and Panstruga, 2012)); and, for *A. thaliana*, the *At4G26410* gene (primers L658-L659, (Hong *et al*., 2010)). The following program was used for amplification: pre-denaturation for 3 min at 94°C, followed by 40 cycles of denaturation for 15 s at 95°C, annealing for 10 s at 62°C and elongation for 10 s at 72°C. Melting curve analysis was performed from 55°C to 95°C, with a step-wise increase of 0.5°C. The amount of the bacterial *16S* rRNA and the *G. orontii*-specific gene was normalized to the reference plant gene within each individual sample using the $2^{-\Delta\Delta Ct}$ equation (Pfaffl, 2001; Weßling and Panstruga, 2012). Absolute abundances of

individual bacteria in SynCom experiments were obtained by multiplying the bacterial gene/plant gene ratio to their individual relative abundances (Wippel *et al*., 2021).

Processing of 16S *gene and* ITS *region amplicon data*

Amplicon sequencing data from the natural soil experiment (plant tissues along with unplanted controls) were demultiplexed according to their barcode sequence using the QIIME pipeline (Caporaso *et al*., 2010). Afterwards, DADA2 (Callahan *et al*., 2016) was used to process the raw sequencing reads of each sample. Unique ASVs were then inferred from trimmed, filtered and error-corrected reads, followed by filtering of chimeric sequences, also using the DADA2 pipeline. Next, ASVs were aligned to the SILVA database (Quast *et al*., 2013) for taxonomic assignment using the naïve Bayesian classifier implemented in DADA2. Subsequently, raw reads were mapped to the inferred ASVs to generate a count table, which was then employed for downstream diversity analyses. *In silico* depletion of *Golovinomyces*-assigned reads was performed by removing ASVs of the *Golovinomyces* genus from the count table, before re-normalization. Then, alpha- and beta-diversity indexes were re-calculated following the steps described below.

Sequencing data from SynCom experiments were processed using the Rbec tool (Zhang *et al*., 2021). First, reads were de-replicated into unique tags that were then aligned to a reference database built from amplicon sequences retrieved from the whole genome sequences of individual SynCom members. Then, initial abundances were assigned to each strain according to the number of reads exactly aligned to each tag. Next, tags that were not exactly matched to any sequence in the database were assigned a candidate error-producing reference based on *k*-mer distances. Sequencing reads were then subsampled and an error matrix was calculated using the mapping between subsampled reads and candidate error-producing sequences. The parameters of the error model were computed iteratively until the number of re-assignments fell below a set threshold. Strain abundances were then estimated from the number of error-corrected reads mapped to each reference sequence. Next, a count table (ASV table) was generated for each strain, normalized by their corresponding *16S* copy number, and subsequently employed for downstream analyses of diversity.

ASV tables and α- and β-diversity metrics

All ASV tables obtained from the pipelines described above were filtered for very low-abundance ASVs before any further analysis. For this, only ASVs with at least 0.1% relative abundance in at least one sample were kept. These filtered tables were used for all further analyses, using the vegan package in R (Oksanen *et al*., 2007). The α-diversity (Shannon) index was calculated using ASV tables rarefied to 1000 reads (*diversity* function). Bray–Curtis distances between samples were calculated using ASV tables that were rarefied to 1000 reads (*vegdist* function). PCoAs were performed using the *cmdscale* function and constrained PCoA analysis using *capscale*. Differential abundance of ASVs was performed using ASV relative abundances and the R package DESeq2 (Love *et al*., 2014). To test for the effect of treatment and compartment on the composition of the bacterial and fungal communities, Bray–Curtis dissimilarity matrices were analysed between pairs of samples with iterations of a permutation-based test using a PERMANOVA model with the *anova.cca* function (R package vegan). Finally, amplicon data from all experiments were visualized using the ggplot2 R package (Wickham, 2016).

Abbreviations

ASV	Amplicon sequence variant
dpi	days post-inculation
ITS	Internal transcribed spacer
PCoA	Principal coordinates analysis
SynCom	Synthetic community

Author Contributions

P.S.-L. and R.P. conceived the project. R.P., P.S.-L. and R.G.-O. designed the experiments. A.L.R., A.R. and M.H. performed the experiments with natural soil. A.L.R., A.R. and P.D. performed the SynCom experiments. P.D. and R.G.-O. analysed the data. P.D. and R.G.-O. created the figures. R.P. and P.S.-L. wrote the manuscript with support from A.R., P.D. and R.G.-O.

Data Availability Statement

Raw demultiplexed sequencing data and corresponding mapping files will be available at ENA accession number PRJEB43139.

References

Acevedo-Garcia, J., Gruner, K., Reinstädler, A., Kemen, A., Kemen, E., Cao, L., *et al*. (2017) The powdery mildew-resistant Arabidopsis *mlo2 mlo6 mlo12* triple mutant displays altered infection phenotypes with diverse types of phytopathogens. *Sci Rep* **7**: 27.

Agler, M.T., Ruhe, J., Kroll, S., Morhenn, C., Kim, S.-T., Weigel, D., and Kemen, E.M. (2016) Microbial hub taxa link host and abiotic factors to plant microbiome variation. *PLoS Biol* **14**: e1002352.

Bai, Y., Müller, D.B., Srinivas, G., Garrido-Oter, R., Potthoff, E., Rott, M., *et al*. (2015) Functional overlap of the *Arabidopsis* leaf and root microbiota. *Nature* **528**: 364–369.

Bazzicalupo, A.L., Bálint, M., and Schmitt, I. (2013) Comparison of ITS1 and ITS2 rDNA in 454 sequencing of hyperdiverse fungal communities. *Fungal Ecol* **6**: 102–109.

Berendsen, R.L., Vismans, G., Yu, K., Song, Y., de Jonge, R., Burgman, W.P., *et al*. (2018) Disease-induced assemblage of a plant-beneficial bacterial consortium. *ISME J* **12**: 1496–1507.

Braun, U., Shin, H.D., Takamatsu, S., Meeboon, J., Kiss, L., Lebeda, A., *et al*. (2019) Phylogeny and taxonomy of *Golovinomyces orontii* revisited. *Mycol Prog* **18**: 335–357.

Bulgarelli, D., Rott, M., Schlaeppi, K., Ver Loren van Themaat, E., Ahmadinejad, N., Assenza, F., *et al*. (2012) Revealing structure and assembly cues for *Arabidopsis* root-inhabiting bacterial microbiota. *Nature* **488**: 91–95.

Bulgarelli, D., Schlaeppi, K., Spaepen, S., Ver Loren van Themaat, E., and Schulze-Lefert, P. (2013) Structure and functions of the bacterial microbiota of plants. *Annu Rev Plant Biol* **64**: 807–838.

Callahan, B.J., McMurdie, P.J., Rosen, M.J., Han, A.W., Johnson, A.J.A., and Holmes, S.P. (2016) DADA2: high-resolution sample inference from Illumina amplicon data. *Nat Methods* **13**: 581–583.

Caporaso, J.G., Kuczynski, J., Stombaugh, J., Bittinger, K., Bushman, F.D., Costello, E.K., *et al*. (2010) QIIME allows analysis of high-throughput community sequencing data. *Nat Methods* **7**: 335–336.

Coleman-Derr, D., Desgarennes, D., Fonseca-Garcia, C., Gross, S., Clingenpeel, S., Woyke, T., et al. (2016) Plant compartment and biogeography affect microbiome composition in cultivated and native Agave species. *New Phytologist* **209**: 798–811.

Dewdney, J., Reuber, T.L., Wildermuth, M.C., Devoto, A., Cui, J.P., Stutius, L.M., Drummond, E.P., and Ausubel, F. M. (2000) Three unique mutants of Arabidopsis identify eds loci required for limiting growth of a biotrophic fungal pathogen. *Plant Journal* **24**: 205–218.

Durán, P., Thiergart, T., Garrido-Oter, R., Agler, M., Kemen, E., Schulze-Lefert, P., and Hacquard, S. (2018) Microbial interkingdom interactions in roots promote Arabidopsis survival. *Cell* **175**: 973–983.e14.

Eichmann, R., and Hückelhoven, R. (2008) Accommodation of powdery mildew fungi in intact plant cells. *J Plant Physiol* **165**: 5–18.

Fabro, G., Di Rienzo, J.A., Voigt, C.A., Savchenko, T., Dehesh, K., Somerville, S., and Alvarez, M.E. (2008) Genome-wide expression profiling Arabidopsis at the stage of *Golovinomyces cichoracearum* haustorium formation. *Plant Physiol* **146**: 1421–1439.

Garrido-Oter, R., Nakano, R.T., Dombrowski, N., Ma, K.-W., McHardy, A.C., and Schulze-Lefert, P. (2018) Modular traits of the rhizobiales root microbiota and their evolutionary relationship with symbiotic rhizobia. *Cell Host Microbe* **24**: 155–167.e5.

Gao, C., Montoya, L., Xu, L., Madera, M., Hollingsworth, J., Purdom, E., et al. (2020) Fungal community assembly in drought-stressed sorghum shows stochasticity, selection, and universal ecological dynamics. *Nature Communications* **11**: 34.

Hacquard, S., and Schadt, C.W. (2015) Towards a holistic understanding of the beneficial interactions across the *Populus* microbiome. *New Phytol* **205**: 1424–1430.

Harbort, C.J., Hashimoto, M., Inoue, H., Niu, Y., Guan, R., Rombolà, A.D., *et al*. (2020) Root-secreted coumarins and the microbiota interact to improve iron nutrition in *Arabidopsis*. *Cell Host Microbe* **28**: 825–837.e6.

Hong, S.M., Bahn, S.C., Lyu, A., Jung, H.S., and Ahn, J.H. (2010) Identification and testing of superior reference genes for a starting pool of transcript normalization in Arabidopsis. *Plant Cell Physiol* **51**: 1694–1706.

Innerebner, G., Knief, C., and Vorholt, J.A. (2011) Protection of *Arabidopsis thaliana* against leaf-pathogenic *Pseudomonas syringae* by *Sphingomonas* strains in a controlled model system. *Appl Environ Microbiol* **77**: 3202–3210.

Jakuschkin, B., Fievet, V., Schwaller, L., Fort, T., Robin, C., and Vacher, C. (2016) Deciphering the pathobiome: intra- and interkingdom interactions involving the pathogen *Erysiphe alphitoides*. *Microb Ecol* **72**: 870–880.

Kuhn, H., Kwaaitaal, M., Kusch, S., Acevedo-Garcia, J., Wu, H., and Panstruga, R. (2016) Biotrophy at its best: novel findings and unsolved mysteries of the Arabidopsis-powdery mildew pathosystem. *Arabidopsis Book* **14**: e0184.

Lebeis, S.L., Paredes, S.H., Lundberg, D.S., Breakfield, N., Gehring, J., McDonald, M., *et al*. (2015) Salicylic acid modulates colonization of the root microbiome by specific bacterial taxa. *Science* **349**: 860–864.

Love, M.I., Huber, W., and Anders, S. (2014) Moderated estimation of fold change and dispersion for RNA-seq data with DESeq2. *Genome Biol* **15**: 550.

Lundberg, D.S., Lebeis, S.L., Paredes, S.H., Yourstone, S., Gehring, J., Malfatti, S., *et al*. (2012) Defining the core *Arabidopsis thaliana* root microbiome. *Nature* **488**: 86–90.

Lyngkjær, H.F., and Carver, T.L.W. (1999a) Modification of *mlo5* resistance to *Blumeria graminis* attack in barley as a consequence of induced accessibility and inaccessibility. *Physiol Mol Plant Pathol* **55**: 163–174.

Lyngkjær, M.F., and Carver, T.L.W. (1999b) Induced accessibility and inaccessibility to *Blumeria graminis* f.sp *hordei* in barley epidermal cells attacked by a compatible isolate. *Physiol Mol Plant Pathol* **55**: 151–162.

Lyngkjær, M.F., Carver, T.L.W., and Zeyen, R.J. (2001) Virulent *Blumeria graminis* infection induces penetration susceptibility and suppresses race-specific hypersensitive resistance against avirulent attack in *Mla1*-barley. *Physiol Mol Plant Pathol* **59**: 243–256.

Malathrakis, N.E. (1985) The fungus *Acremonium alternatum* Linc:Fr., a hyperparasite of the cucurbits powdery mildew pathogen *Sphaerotheca fuliginea*. *Z Pflanzenkr Pflanzenschutz-J Plant Dis Prot* **92**: 509–515.

Müller, D.B., Vogel, C., Bai, Y., and Vorholt, J.A. (2016) The plant microbiota: systems-level insights and perspectives. *Annu Rev Genet* **50**: 211–234.

Oksanen, J., Kindt, R., Legendre, P., O'Hara, B., Stevens M. H.H., and Oksanen, M.J. (2007) The vegan package: community ecology package. *R package version*.

Panstruga, R., and Kuhn, H. (2019) Mutual interplay between phytopathogenic powdery mildew fungi and other microorganisms. *Mol Plant Pathol* **20**: 463–470.

Pfaffl, M.W. (2001) A new mathematical model for relative quantification in real-time RT-PCR. *Nucleic Acids Res* **29**: e45.

Poraty-Gavra, L., Zimmermann, P., Haigis, S., Bednarek, P., Hazak, O., Stelmakh, O.R., et al. (2013) The Arabidopsis Rho of plants GTPase AtROP6 functions in developmental and pathogen response pathways. *Plant Physiology* **161**: 1172–1188.

Quast, C., Pruesse, E., Yilmaz, P., Gerken, J., Schweer, T., Yarza, P., *et al*. (2013) The SILVA ribosomal RNA gene database project: improved data processing and web-based tools. *Nucleic Acids Res* **41**: D590–D596.

Russ, L., Lombaers-van der Plas, C., Castillo-Russi, J.D., Zijlstra, C., and Köhl, J. (2021) Deciphering the modes of action of *Golubevia sp*., an antagonist against the causal agent of powdery mildew in wheat, using an mRNA-based systems approach. *Biol Control* **152**: 104446.

Schlaeppi, K., Dombrowski, N., Oter, R.G., van Loren ver Themaat, E., and Schulze-Lefert, P. (2014) Quantitative divergence of the bacterial root microbiota in *Arabidopsis thaliana* relatives. *Proc Natl Acad Sci U S A*, **111**: 585–592.

Schulze-Lefert, P., and Panstruga, R. (2003) Establishment of biotrophy by parasitic fungi and reprogramming of host cells for disease resistance. *Annu Rev Phytopathol* **41**: 641–667.

Seybold, H., Demetrowitsch, T.J., Hassani, M.A., Szymczak, S., Reim, E., Haueisen, J., *et al*. (2020) A fungal pathogen induces systemic susceptibility and systemic shifts in wheat metabolome and microbiome composition. *Nat Commun* **11**: 1910.

Singh, U.P., and Mishra, G.D. (1992) Effect of powdery mildew (*Erysiphe pisi*) on nodulation and nitrogenase activity in pea (*Pisum sativum*). *Plant Pathol* **41**: 262–264.

Snelders, N.C., Kettles, G.J., Rudd, J.J., and Thomma, B.P. H.J. (2018) Plant pathogen effector proteins as manipulators of host microbiomes? *Mol Plant Pathol* **19**: 257–259.

Snelders, N.C., Rovenich, H., Petti, G.C., Rocafort, M., van den Berg, G.C.M., Vorholt, J.A., *et al*. (2020) Microbiome manipulation by a soil-borne fungal plant pathogen using effector proteins. *Nat Plants* **6**: 1365–1374.

Spanu, P.D., Abbott, J.C., Amselem, J., Burgis, T.A., Soanes, D.M., Stüber, K., *et al*. (2010) Genome expansion and gene loss in powdery mildew fungi reveal tradeoffs in extreme parasitism. *Science* **330**: 1543–1546.

Stein, E., Molitor, A., Kogel, K.-H., and Waller, F. (2008) Systemic resistance in Arabidopsis conferred by the mycorrhizal fungus Piriformospora indica requires jasmonic acid signaling and the cytoplasmic function of NPR1. *Plant and Cell Physiology* **49**: 1747–1751.

Swarbrick, P.J., Schulze-Lefert, P., and Scholes, J.D. (2006) Metabolic consequences of susceptibility and resistance (race-specific and broad-spectrum) in barley leaves challenged with powdery mildew. *Plant Cell Environ* **29**: 1061–1076.

Thiergart, T., Durán, P., Ellis, T., Vannier, N., Garrido-Oter, R., Kemen, E., *et al*. (2020) Root microbiota assembly and adaptive differentiation among European Arabidopsis populations. *Nat Ecol Evol* **4**: 122–131.

Vogel, C., Bodenhausen, N., Gruissem, W., and Vorholt, J. A. (2016) The Arabidopsis leaf transcriptome reveals distinct but also overlapping responses to colonization by phyllosphere commensals and pathogen infection with impact on plant health. *New Phytol* **212**: 192–207.

Vorholt, J.A. (2012) Microbial life in the phyllosphere. *Nat Rev Microbiol* **10**: 828–840.

Wagner, M.R., Lundberg, D.S., Del Rio, T.G., Tringe, S.G., Dangl, J.L., and Mitchell-Olds, T. (2016) Host genotype and age shape the leaf and root microbiomes of a wild perennial plant. *Nat Commun* **7**: 12151.

Weßling, R., and Panstruga, R. (2012) Rapid quantification of plant-powdery mildew interactions by qPCR and conidiospore counts. *Plant Methods* **8**: 35.

Wickham, H. (2016) ggplot2. In *Elegant Graphics for Data Analysis*. Cham: Springer International Publishing.

Wippel, K., Tao, K., Niu, Y., Zgadzaj, R., Guan, R., Dahms, E., *et al*. (2021) Host preference and invasiveness of commensals in the *Lotus* and *Arabidopsis* root microbiota. *bioRxiv* **6**: 1150–1162.

Wright, D.P., Baldwin, B.C., Shephard, M.C., and Scholes, J. D. (1995) Source-sink relationships in wheat leaves infected with powdery mildew. I. Alterations in carbohydrate metabolism. *Physiol Mol Plant Pathol* **47**: 237–253.

Yamaoka, N., Toyoda, K., Kobayashi, I., and Kunoh, H. (1994) Induced accessibility and enhanced inaccessibility at the cellular level in barley coleoptiles .13. Significance of haustorium formation by the pathogen *Erysiphe graminis* for induced accessibility to the non-pathogen *E. pisi* as asessed by nutritional manipulations. *Physiol Mol Plant Pathol* **44**: 217–225.

Yang, R.-H., Su, J.-H., Shang, J.-J., Wu, Y.-Y., Li, Y., Bao, D.-P., and Yao, Y.-J. (2018) Evaluation of the ribosomal DNA internal transcribed spacer (ITS), specifically ITS1 and ITS2, for the analysis of fungal diversity by deep sequencing. *PLoS One* **13**: e0206428.

Zhang, J., Liu, Y.-X., Zhang, N., Hu, B., Jin, T., Xu, H., *et al*. (2019a) NRT1.1B is associated with root microbiota composition and nitrogen use in field-grown rice. *Nat Biotechnol* **37**: 676–684.

Zhang, P., Spaepen, S., Bai, Y., Hacquard, S., and Garrido-Oter, R. (2021) Reference-based error correction of amplicon sequencing data from synthetic communities. *bioRxiv*. https://doi.org/10.1101/2021.01.15.426834

Zhang, Z., Kong, X., Jin, D., Yu, H., Zhu, X., Su, X., *et al*. (2019b) *Euonymus japonicus* phyllosphere microbiome is significantly changed by powdery mildew. *Arch Microbiol* **201**: 1099–1109.

Zhang, Z., Luo, L., Tan, X., Kong, X., Yang, J., Wang, D., *et al*. (2018) Pumpkin powdery mildew disease severity influences the fungal diversity of the phyllosphere. *PeerJ* **6**: e4559.

Supporting Information

Additional Supporting Information may be found in the online version of this article at the publisher's web-site:

Supplementary Fig. 1 Changes in relative abundance of bacterial ASVs in *A. thaliana* leaves upon *G. orontii* infection. Each bacterial ASV that showed significant enrichment in leaf samples inoculated with *G. orontii*, compared to non-inoculated samples ($P < 0.05$, DESeq package in R) is

shown. Each row represents a different ASV, where the size of each dot corresponds to the log-transformed relative abundance in a given sample (columns). The dots are colour-coded based on the ASV taxonomic assignment at the class level. The right panel depicts the fold change of each significantly enriched ASV in *G. orontii*-inoculated leaves, compared to non-inoculated control leaves.

Supplementary Fig. 2. Changes in relative abundance of fungal ASVs in *A. thaliana* leaves upon *G. orontii* colonization, for the *ITS1* community profiles. Each fungal ASV that showed significant enrichment in leaf samples inoculated with *G. orontii*, compared to non-inoculated samples ($P < 0.05$, DESeq package in R) is shown here. Each row represents a different ASV, where the size of each dot corresponds to the log-transformed relative abundance in a given sample (columns). The dots are colour-coded based on the ASV taxonomic assignment at the class level. The right panel depicts the fold change of each significantly enriched ASV in *G. orontii*-inoculated leaves, compared to non-inoculated control leaves.

Supplementary Fig. 3. Changes in relative abundance of fungal ASVs in *A. thaliana* leaves upon *G. orontii* infection, for the *ITS2* community profiles. Each fungal ASV that showed significant enrichment in leaf samples inoculated with *G. orontii*, compared to non-inoculated samples ($P < 0.05$, DESeq package in R) is shown here. Each row represents a different ASV, where the size of each dot corresponds to the log-transformed relative abundance in a given sample (columns). The dots are colour-coded based on the ASV taxonomic assignment at the class level. The right panel depicts the fold change of each significantly enriched ASV in *G. orontii*-inoculated leaves, compared to non-inoculated control leaves.

Supplementary Fig. 4. Heatmap of bacterial strain-specific relative abundance including SynCom samples (Root *At*-SPHERE strains). Warm colours correspond to abundant strains detected in at least one input sample (>0.1% relative abundance). Samples (columns) are grouped by compartment and *G. orontii* treatment.

Supplementary Fig. 5. Heatmap of bacterial strain-specific relative abundances including SynCom samples (Leaf *At*-SPHERE strains). Warm colours correspond to abundant strains detected in at least one input sample (>0.1% relative abundance). Samples (columns) are grouped by compartment and *G. orontii* treatment.

Supplementary Fig. 6. Comparison of absolute abundances of individual Leaf *At*-SPHERE bacteria to relative abundances in the culture-independent approach. A) Absolute abundance (shown as the product of the bacterial/plant gene ratio multiplied with the bacterial relative abundance of each bacterial strain from the Leaf *At*-SPHERE inoculated in *A. thaliana* leaves in the absence or presence of *G. orontii*. Boxplots are colour-coded based on the taxonomic assignment of each strain at the class level. Significant differences in absolute abundances upon *G. orontii* inoculation are depicted with a red asterisk (Student's *t*-test, $P < 0.05$, FDR corrected). B) Aggregated relative (culture-independent approach; plants grown in natural soil – Fig. 1A) and absolute (culture-dependent approach; SynCom experiments – Fig. 4A) abundances of bacterial orders shared between the two experimental set-ups. Significant differences in abundances upon *G. orontii* inoculation are depicted with a red asterisk (Student's *t*-test, $P < 0.05$, FDR corrected).

Supplementary Fig. 7. Profiling of *G. orontii* inoculum. A) Number of reads assigned to either bacterial or fungal ASVs in *A. thaliana* leaves inoculated with *G. orontii* B) Relative abundances of bacterial ASVs colour-coded based on their taxonomic assignment at the class level. C) Relative abundances of fungal ASVs from the *ITS1* profiles, colour-coded based on their taxonomic assignment at the genus level. D) Relative abundances of fungal ASVs from the *ITS2* profiles, colour-coded based on their taxonomic assignment at the genus level.

Supplementary Table 1.

List of Root *At*-SPHERE strains used in this study and their taxonomic assignment

List of Leaf *At*-SPHERE strains used in this study and their taxonomic assignment

Primers used in library preparation for amplicon sequencing

Sequencing primers used for MiSeq sequencing

Natural soil experiment mapping file for the analysis of community profiles

SynCom experiments mapping file for the analysis of community profiles

Primers used in qPCR for microbial absolute quantification in plant tissues

Number of samples in the various experiments